PHYSICAL REVIEW B

CONDENSED MATTER AND MATERIALS PHYSICS

THIRD SERIES, VOLUME 59, NUMBER 13 **1 APRIL 1999-I**

BRIEF REPORTS

Brief Reports are accounts of completed research which, while meeting the usual **Physical Review B** *standards of scientific quality, do not warrant regular articles. A Brief Report may be no longer than four printed pages and must be accompanied by an abstract. The same publication schedule as for regular articles is followed, and page proofs are sent to authors.*

NMR and high-resolution x-ray diffraction evidence for an alkali-metal fulleride with large interstitial clusters: $Li_{12}C_{60}$

Luigi Cristofolini, Mauro Riccò, and Roberto De Renzi

Dipartimento di Fisica and Istituto Nazionale di Fisica della Materia, Viale delle Scienze 7,A, I-43100 Parma, Italy

(Received 9 June 1998; revised manuscript received 2 November 1998)

NMR and high-resolution x-ray diffraction of several lithium-doped fullerides Li_xC_{60} show that the stoichiometry $x=12$ represents a stable Li doping for a high symmetry C_{60}-like phase, which might extend to much larger x. $Li_{12}C_{60}$ is fcc at high temperature, and it distorts to tetragonal upon cooling. We have evidence from ^{13}C NMR that the C_{60} units are static in the tetragonal phase at least up to $T=373$ K. Rietvelt refinement of the fcc phase favors a hybrid cluster intercalated structure with shortening of selected Li-C distances. [S0163-1829(99)00414-2]

The intercalation of fullerene by large radius alkali metals ($A=$K,Rb,Cs; ionic radii $=1.33,1.47,1.67$ Å, respectively) yields salts of stoichiometry A_xC_{60} ($x=1,3,4,6$; $A=$K,Rb,Cs). Among these compositions both superconductors ($x=3$) and magnetic materials ($x=1$) are found. The structure of all of these compounds, with the only notable exception of A_1C_{60} in the low-temperature phases, can be rationalized in terms of rigid spheres (the alkali-metal ions) progressively filling the voids of the pristine cubic fullerene structure. The pseudocubic lattice constant expands to accommodate the larger radius alkali metal. A natural limit in the doping level is reached at $x=6$ due to the complete occupancy of the voids of the cubic structure.

There is renewed interest in small radius alkali-metal fullerides since the observation of superconductivity in Li_xCsC_{60} ($3<x<4$).[1] Li and Na (ionic radii$=0.63,0.97$ Å, respectively) may also yield phases with higher alkali-metal content, due to the tendency to form metallic clusters located in the voids of the pseudocubic fullerene structure, as is the case of $Na_{11}C_{60}$.[2,3] In binary doped fullerides as $A_xA'_{3-x}C_{60}$ ($A=$Na,Li, $A'=$K,Rb,Cs) sodium and lithium have the tendency to move from the center of the voids to partially coordinate with the C_{60} electronic cloud, as it was shown by NMR (Ref. 4) and synchrotron-radiation diffraction[5] (SRD) in Na_2RbC_{60} and by SRD (Ref. 6) in Li_2CsC_{60}.

Early in the history of fullerenes Kohanoff *et al.*,[7] based on Car-Parrinello first-principles molecular-dynamics calculations, proposed that $Li_{12}C_{60}$ could be a stable, highly symmetric fullerene cluster, a ''superfulleroid,'' with the 12 Li ions coordinated with the 12 pentagonal faces of C_{60} thus preserving the icosahedral I_h symmetry. This prediction was supported by mass spectroscopy observations of $Li_{12}C_{60}$ among the different Li_xC_{60} clusters produced in the gas phase.[8] To the best of our knowledge no subsequent experimental confirmation was given about the stability of the $Li_{12}C_{60}$ cluster in the solid state.

Li is the least studied among alkali metals as fullerene dopands, due to preparation difficulties posed by the very low vapor pressure of Li (10^{-9} torr at $T=200\,^{\circ}$C, compared to 10^{-4} torr for Na). Alternatives to the inefficient production by vapor transport of Li to the C_{60} phase are represented by (a) reaction in liquid ammonia, and (b) thermal decomposition of alkali-metal azides. We have employed the latter technique, since the former inevitably leaves traces of ammonia trapped in the solid, originating structural distortions.

The samples were prepared by mixing and pelletizing stoichiometric quantities of purified C_{60} and Li azide LiN_3 in an Ar glove box. The pellets were sealed in an iron foil and placed in high dynamic vacuum. The azide was decomposed by a very slow temperature ramp (5 K/h), the decomposition

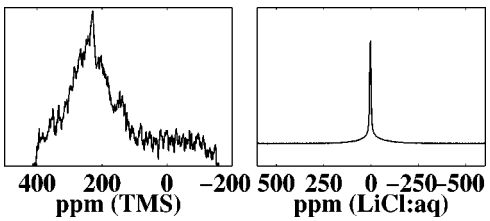

FIG. 1. Left: ^{13}C NMR spectrum of $Li_{12}C_{60}$ at $T=373$ K. Right: ^{7}Li NMR spectrum of $Li_{12}C_{60}$ at RT.

reaction $LiN_3 \rightarrow Li + \frac{3}{2}N_2$ being monitored with a vacuum gauge. The crystallinity was improved by a moderate annealing (typically 6 h at 550 K); neither longer times nor higher temperatures produced further improvement. Preliminary characterization was performed at room temperature on a Siemens D-500 diffractometer (Cu$K\alpha$ radiation). The solid state NMR experiments were performed in the temperature range 110–373 K on a Bruker CXP200 spectrometer ($H_0 = 4.7$ T).

The high-resolution diffraction experiment was performed on the beam line BM16 of European Synchrotron Radiation Facility (ESRF) operating at fixed wavelength [$\lambda = 0.652924(2)$ Å from standard Si calibration]. The sample temperature was stabilized (± 0.1 K) either in cold nitrogen or in a hot air flow, and the capillary was spun around its axis to average out the effect of preferred orientations. Data were simultaneously collected by an array of nine detectors separated by 2° each, which continuously scanned the 2θ region of interest. Data were subsequently rebinned, resummed, and normalized with ESRF software.

We performed preliminary magnetic, NMR, and structural characterization of a series of samples, focusing in particular on the composition $Li_{12}C_{60}$. Superconducting quantum interference device (SQUID) magnetometry showed no trace of either superconducting or magnetic order transitions down to 4.2 K. Up to 373 K the ^{13}C NMR spectrum (Fig. 1, left) shows the full chemical shift anisotropy (about 180 ppm) typical of static fullerides, indicating that the C_{60} rotational dynamic is frozen on the NMR time scale.

The ^{7}Li NMR spectrum at room temperature (Fig. 1, right) consists of a single narrow resonance, with full width at half maximum of 11 ppm and a line shift of $+3$ ppm with respect to the LiCl:aq resonance. The shift is characteristic of Li nuclei in nonmetallic states. No further signal is detected in the spectral region extending up to 1500 ppm, while bulk

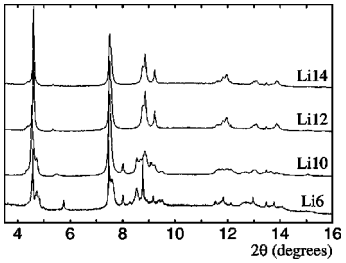

FIG. 2. BM16 Diffraction patterns at room temperature on (from bottom to top) Li_6C_{60}, $Li_{10}C_{60}$, $Li_{12}C_{60}$, and $Li_{14}C_{60}$. Note the similarity between the patterns of $Li_{12}C_{60}$ and $Li_{14}C_{60}$, and the splitting of the (1,1,1) reflection at $2\theta \simeq 4.6°$ in $Li_{10}C_{60}$.

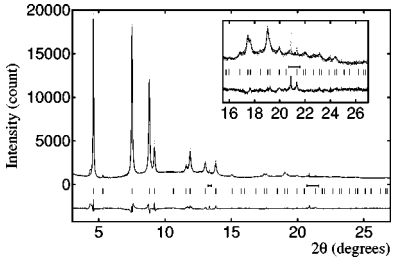

FIG. 3. Diffraction pattern at $T=553.0$ K, $\lambda = 0.652924$ Å (dots), its Rietveld refinement (line) and residues (vertical bars mark the Bragg reflection). Inset: expanded high angle region.

metallic Li is expected at $K \simeq 930$ ppm. This is a clear indication that (a) Li is not segregated in a metallic form, and (b) if Li clusters are present in $Li_{12}C_{60}$, they do not have metallic character. Incidentally, no NMR signal from metallic Li is found up to the highest studied doping level $Li_{24}C_{60}$.

Figure 2 shows the low 2θ portion of the room-temperature (RT) diffraction patterns from different Li_xC_{60} compositions collected on BM16. Note the similarity between the patterns of $Li_{12}C_{60}$ and $Li_{14}C_{60}$, both showing a single (1,1,1) pseudocubic reflection at $2\theta \simeq 4.6°$, although with slightly different distribution of intensities between low and high angle reflections. The $Li_{10}C_{60}$ pattern instead shows a composite structure in place of the single (1,1,1) peak and major differences in the 2θ region 8.5°–10°; Li_6C_{60} shows a completely different pattern. Preliminary laboratory x-ray diffractograms collected on Li_xC_{60} for $12 \leqslant x \leqslant 24$, are identical to that of $Li_{12}C_{60}$. These diffraction patterns and the absence of a bulk metallic lithium NMR signal indicate that for $x \geqslant 12$ we have a single C_{60}-like phase, while for $x < 12$ we have lower symmetry phases and/or a mixture of phases. We never detected any excess Li escaping the reaction (when this happens the sample vessels become metallized), therefore we assume that all the $x \geqslant 12$ compositions are indeed formed. In the following we have focused our attention on the sole $Li_{12}C_{60}$.

The diffraction pattern collected on BM16 at $T=553$ K can be indexed in face-centered cubic symmetry $Fm\bar{3}m$ (fcc) (Fig. 3). The regions $13.25° < 2\theta < 13.50°$ and $20.70° < 2\theta < 21.60°$ contain narrow impurity peaks, excluded from the analysis. The PROFIL (Ref. 9) suite of programs was employed, with a modification[10] which models the C_{60} scattering density in terms of symmetry adapted spherical harmonic (SASH) functions.[11] The $m\bar{3}m$ symmetry of the C_{60} site in

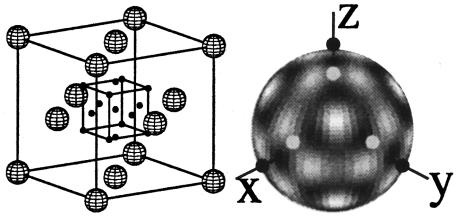

FIG. 4. Left: The structural cell at $T=553$ K (c is the vertical axis). C_{60}: larger spheres (radii not to scale); Li: filled circles. Right: fitted SASH model of C_{60} unit with Li atoms in sites $32f$ and $24e$ (white and black filled circles, respectively).

the fcc lattice implies that only the SASH function coefficients $C_{l,\nu}$ with $l=0,6,10,12$ and $\nu=1$ (plus the term with $l=12$ and $\nu=2$) are nonzero. The $l=0$ term corresponds to the spherical contribution. Different models were tried, both with the superfulleroid structure[7] and in the class of the intercalation compounds with an alkali-metal cluster in the octahedral void, in analogy with $Na_{11}C_{60}$.[2]

Considering the rotational disorder of both C_{60} molecules and Li atoms in the superfulleroid structure, its refinement is implemented by modeling the C_{60} unit as a simple sphere centered at the origin of the $Fm\bar{3}m$ cell, with a starting radius value of $R=3.55$ Å. The 12 Li atoms are placed on second concentric sphere with a starting radius $R=5.1$ Å, such that the C-Li distance is the same as in the superfulleroid model.[7] Both the two radii and the Li occupancy were varied in the fit procedure. This model gave invariably a poor fit ($R_{wp}=19.3\%, R_I=8.1\%, R_{\rm exp}=2.4\%$).

We obtained much better results with an intercalation structure. Figure 3 shows the best fit ($R_{wp}=10.9\%, R_I=6.9\%, R_{\rm exp}=2.5\%$), obtained in the $Fm\bar{3}m$ symmetry shown in Fig. 4, with the C_{60} units modeled as symmetry adapted spherical harmonic functions (SASH) of radius $R=3.559(2)$ Å, centered in $4a$ (0,0,0). This value of R is larger than that found in neutral C_{60} $R=3.5429(6)$,[12] but fully consistent with the radius $R=3.556(4)$ (Ref. 6) of Li_2CsC_{60}. It is indicative of a lengthening of the double bonds as a consequence of the charge transfer onto the C_{60} molecule.

The best fit SASH coefficients are $C_{0,1}=1.0, C_{6,1}=0.038(4), C_{10,1}=0.226(27)$. The coefficients of higher order $C_{12,\nu}$ have little effect on the quality of the fit, hence they were fixed to zero. The resulting density of carbon on the C_{60} sphere (see Fig. 4, right panel) is maximum in the lattice directions (1,0,0) and $(\frac{1}{2},\frac{1}{2},1)$, while it is minimum in the (1,1,1) direction which points towards the tetrahedral void. In Li_2CsC_{60},[6] *vice versa*, the negative $C_{10,1}$ value implies an excess of carbon density in the (1,1,1) direction, which corresponds to Li ions residing in the tetrahedral void.

The Li ions are localized in a cluster located at the octahedral void, while the tetrahedral void $8c$ refines to zero Li occupancy $[N=-0.5(5)]$. The refined Li sites are (i) the centers of the octahedral voids of the cubic structure [sites $4b$ $(\frac{1}{2},\frac{1}{2},\frac{1}{2})$] which refines to almost full occupancy $N=3.2(2)$; (ii) the corners of a cube centered in the octahedral voids [sites 32 f (x,x,x) $x=0.662(1)$] which refines to full occupancy 32(1); (iii) the centers of the faces of the above-mentioned cube [sites $24e$ $(\frac{1}{2},\frac{1}{2},y)$ $y=0.690(1)$], with partial occupancy $N=11.3(7)$.

The isotropic thermal displacement, fitted as a single common value for all the Li atoms, is $B_{\rm iso}=6.6(1.2)$ Å^2 [the isotropic mean-square displacement is $\overline{u^2}=B/(8\pi^2)$]. The total refined Li occupancy [11.6(5) Li per C_{60} unit] is consistent with the nominal stoichiometry $Li_{12}C_{60}$.

We note that the partial random occupancy of sites $24e$ may allow the accomodation of more than 12 Li atoms in the lattice without an appreciable change in lattice parameters. This is in agreement with the observed similarity among the diffraction patterns for $x\geqslant 12$.

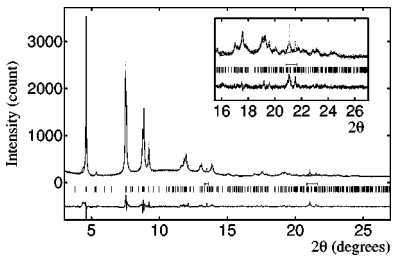

FIG. 5. Diffraction pattern of $Li_{12}C_{60}$ at $T=293.0$ K, $\lambda=0.652924$ Å (dots) with its LeBail fit (line) and the residues (below, with vertical bars at the Bragg reflections); Inset: expanded high-angle region.

Another interesting feature of this model is that there is an excess carbon density on the C_{60} sphere in the directions pointing towards all the Li sites and a minimum carbon density in the (1,1,1) direction corresponding to zero occupancy for the $(\frac{1}{4},\frac{1}{4},\frac{1}{4})$ tetrahedral site. This is an indication of the presence of attractive C-Li interactions. Moreover the Li ion in the site $24e$ (black spheres in Fig. 4, fractional occupancy $\simeq\frac{1}{2}$) is just 0.8 Å apart from the nearest C_{60} unit, thus strongly suggesting the existence of a Li-C bond in this direction. On the contrary the Li ion in the site $32f$ (white spheres in Fig. 4) is 2.2 Å distant from the next C_{60} unit, excluding the presence of a bond for Li in this site. The Li-Li distances, ranging from 2.7 Å for Li(1)–Li(3), to 3.9 Å for Li(1)–Li(3), exclude the presence of Li-Li bonds.

Inspection of the profiles collected at temperatures $T\leqslant 523$ K shows a splitting of the pseudocubic reflections which can be indexed in tetragonal symmetry. The splitting increases as the temperature is lowered. Starting the fit from a cubic cell of lattice parameter a', we have chosen the tetragonal unit cell with $a=a'/\sqrt{2}, c=a'$. This choice identifies directly the parameter a with the closest distance between the C_{60} units.

All detected low-angle reflections follow the rule $(h+k+l=2n)$, although a few exceptions are found at high angles [namely (4,2,1) at $2\theta=17.18°$, (5,1,1) at $2\theta=19.56°$]. This suggests a small distortion of the bct cell towards primitive tetragonal, possibly by a displacement of the C_{60} unit from the symmetric $(\frac{1}{2},\frac{1}{2},\frac{1}{2})$ site.

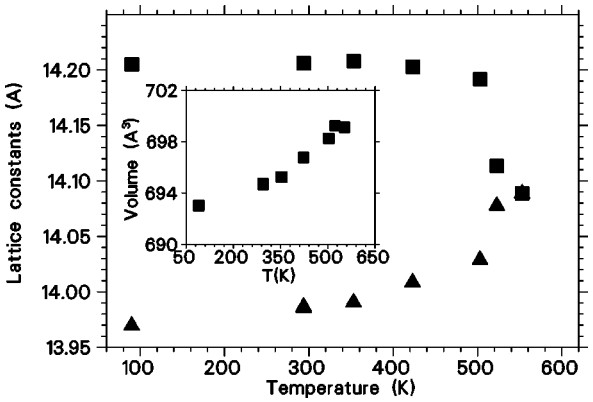

FIG. 6. Temperature dependence of the $Li_{12}C_{60}$ lattice parameters c (squares) and a, scaled by $\sqrt{2}$ (triangles); Inset: unit volume (Å^3) as a function of temperature.

Figure 5 shows the room-temperature profile of $Li_{12}C_{60}$ together with its best fit by the LeBail[13] pattern decomposition technique with pseudo-Voigt peak functions [$a=b=9.894(1)$ Å, $c=14.209(1)$ Å, quality of the fit: $R_{wp}=12.89\%$, $R_{\exp}=3.7\%$, $R_I=0.3\%$]. The shoulder on the low angle side of the (1,1,1) reflection at $2\theta=4.60°$ is not uncommon in fullerene diffraction patterns and may be ascribed either to stacking faults or to a minority hexagonal phase. There are a couple of small narrow impurity peaks at $2\theta\approx13.5°$ and $2\theta\approx20.9°$ similar to those found at higher temperatures. They were excluded from the analysis.

The temperature dependence of the lattice parameters and the unit-cell volume extracted by the LeBail technique are shown in Fig. 6. Although the LeBail fit is clearly not a full structural refinement it allows a reliable determination of the cell volume both at low and at high temperature. $Li_{12}C_{60}$ has a much smaller unit volume than C_{60} ($V=710$ Å^3),[12] and the A_xC_{60} (e.g., $V=724$ Å^3 in K_3C_{60}).[14] A similar reduced value is found in Li_2CsC_{60} ($V=697.0$ Å^3 at RT)[6] where the Cs^+ cations occupy the large octahedral void and the small Li^+ cations reside in the tetrahedral voids. The reduction of V with respect to C_{60} may be due to the electrostatic attraction between C_{60}^{n-} anions and the alkali-metal cations. The same phenomenon should take place also in the A_3C_{60} salts (A=K,Rb,Cs) where it is however contrasted by the steric hindrance due to the large cations. $Li_{12}C_{60}$ may then be regarded as the fullerene-alkali metal compound with the highest C_{60} volume packing.

In conclusion we have shown that Li doping of fullerene results in a single phase Li_xC_{60} for $x\geqslant12$. The upper limit for the existence of this phase is still to be investigated, but we have evidence that it lies above $x=24$. $Li_{12}C_{60}$ has cubic symmetry at 553 K and distorts to tetragonal symmetry upon cooling. We have NMR evidence that the C_{60} units are static in the tetragonal phase at least up to $T=373$ K.

The structure of $Li_{12}C_{60}$ is that of an intercalation compound with all the Li ions concentrated in the octahedral void of the fullerene pseudocubic structure. We have strong indications of coordination between most of the Li ions and the carbon density on the nearest C_{60} unit. The emerging picture at high temperature is thus of an hybrid between the superfulleroid cluster[7] and a conventional intercalation compound such as K_3C_{60}. A simple superfulleroid model is ruled out by our refinements at $T=513$ K, although this could just be due to a high-temperature dissociation, or possibly to solid state effects on this cluster, not included in the original calculations[7].

The authors gratefully acknowledge the BM16 staff (Eric Doorhyee and Andy Fitch) for invaluable experimental help, Wanda Andreoni and Kosmas Prassides for useful discussions, K.P. also for providing us with the code for the SASH analysis, Fulvio Bolzoni for the SQUID measurements, and Marco Fontana for continuous support.

[1] M. Kosaka, K. Tanigaki, and K. Prassides, in *Proceedings of the Symposium on Recent Advances in the Chemistry and Physics of Fullerenes and Related Materials*, San Diego, 1998, edited by K. M. Kadish and R. Ruoff (The Electrochemical Society, Pennington, New Jersey, 1998).

[2] T. Yildirim, O. Zhou, J. E. Fischer, N. Bykovetz, R. A. Strongin, M. A. Cichy, A. B. Smith, C. L. Lin, and R. Jelinek, Nature (London) **360**, 568 (1992).

[3] W. Andreoni, P. Giannozzi, J. F. Armbruster, M. Knupfer, and J. Fink, Europhys. Lett. **34**, 699 (1996).

[4] L. Cristofolini, K. Kordatos, G. A. Lawless, K. Prassides, K. Tanigaki, and M. P. Waugh, J. Chem. Soc. Chem. Commun. **4**, 375 (1997).

[5] K. Prassides, K. Vavekis, K. Kordatos, K. Tanigaki, G. M. Bendele, and P. W. Stephens, J. Am. Chem. Soc. **119**, 834 (1997).

[6] I. Hirosawa, K. Prassides, J. Mizuki, K. Tanigaki, M. Gevaert, A. Lappas, and J. K. Cockcroft, Science **264**, 1294 (1994).

[7] J. Kohanoff, W. Andreoni, and M. Parrinello, Chem. Phys. Lett. **198**, 472 (1992); (private communication).

[8] T. P. Martin, N. Malinowski, U. Zimmermann, U. Näher, and H. Schaber, J. Chem. Phys. **99**, 4210 (1993).

[9] PROFIL, 5.17; J. K. Cockcroft, Birbeck College, London, 1997.

[10] K. Prassides (private communication).

[11] W. Press and A. Huller, Acta Crystallogr. Sect. A **29**, 252 (1973); J. P. Amoreaux and M. Bee, Acta Crystallogr., Sect. B **36**, 2636 (1980); J. K. Cockroft and A. Fitch, Z. Kristallogr. **184**, 123 (1988).

[12] P. C. Chow, X. Jiang, G. Reiter, P. Wochner, S. C. Moss, J. D. Axe, J. C. Hanson, R. K. McMullan, R. L. Meng, and C. W. Chu, Phys. Rev. Lett. **69**, 2943 (1992).

[13] A. LeBail, H. Duroy, and J. L. Fouquet, Mater. Res. Bull. **23**, 447 (1988).

[14] P. W. Stephens, L. Mihaly, P. L. Lee, R. L. Whetten, S. M. Huang, R. Kaner, F. Diederich, and K. Holczer, Nature (London) **351**, 632 (1991).